

Kinetic and thermodynamic analyses of the corrosion inhibition of synthetic extracellular polymeric substances

Liew Chien Go¹, Dilip Depan¹, William Holmes², August Gallo³, Kathleen Knierim³, Tre Bertrand⁴, Rafael Hernandez^{Corresp. 1, 2}

¹ Department of Chemical Engineering, University of Louisiana at Lafayette, Lafayette, Louisiana, United States

² Energy Institute of Louisiana, University of Louisiana at Lafayette, Lafayette, Louisiana, United States

³ Department of Chemistry, University of Louisiana at Lafayette, Lafayette, Louisiana, United States

⁴ Coastal Chemical Co. LLC, Broussard, Louisiana, United States

Corresponding Author: Rafael Hernandez
Email address: rafael.hernandez@louisiana.edu

Background. Extracellular polymeric substances (EPS) extracted from waste activated sludge (WAS) have previously shown its potential in corrosion inhibition. The aim of this study is to design a synthetic EPS formulation as a surrogate of natural WAS EPS to overcome the corrosion inhibition inconsistency in WAS EPS. The adsorption behavior of the designed inhibitor was studied by kinetic and thermodynamic analyses.

Methods. Synthetic EPS is a bio-inspired material that was formulated based on the most typical chemical compositions of natural WAS EPS, i.e. proteins, carbohydrates, humic substances, nucleic acids, and uronic acids, which was not optimized for corrosion inhibition performance. It is a mixture of glutamic acid, carboxymethylcellulose, humic acid, thymine, and alginic acid. Its corrosion inhibition performance was tested with carbon steel in 3.64% NaCl saturated with CO₂, using the potentiodynamic polarization scanning technique. The resulted electrochemical parameters were used to evaluate the empirical corrosion kinetic and thermodynamic adsorption parameters.

Results. Addition of synthetic EPS showed significant decrease in corrosion rate as compared to the control. The inhibition efficiency improved with increasing inhibitor concentration and temperature. The optimum performance was 94% with 204 mg/L of inhibitor applied at 70°C (343 K). The inhibition performance was controlled by both the concentration of inhibitor and temperature. Chemisorption of the inhibitor molecules contributed to the overall inhibition performance, reducing the contact of metal with the corrosive environment, thus, slowing down the overall corrosion rate.

1 **Kinetic and thermodynamic analyses of the corrosion**
2 **inhibition of synthetic extracellular polymeric**
3 **substances**

4

5 Liew Chien Go¹, Dilip Depan¹, William Holmes², August Gallo³, Kathleen Knierim³, Tre
6 Bertrand⁴, Rafael Hernandez^{1,2}

7

8 ¹ Department of Chemical Engineering, University of Louisiana at Lafayette, Lafayette,
9 Louisiana, United States

10 ² Energy Institute of Louisiana, University of Louisiana at Lafayette, Lafayette, Louisiana,
11 United States

12 ³ Department of Chemistry, University of Louisiana at Lafayette, Lafayette, Louisiana, United
13 States

14 ⁴ Coastal Chemical Co., LLC, Broussard, Louisiana, United States

15

16 Corresponding Author:

17 Rafael Hernandez^{1,2}

18 131 Rex Street, Lafayette, LA, 70503, USA

19 Email address: rafael.hernandez@louisiana.edu

20 Abstract

21 **Background.** Extracellular polymeric substances (EPS) extracted from waste activated sludge
22 (WAS) have previously shown its potential in corrosion inhibition. The aim of this study is to
23 design a synthetic EPS formulation as a surrogate of natural WAS EPS to overcome the
24 corrosion inhibition inconsistency in WAS EPS. The adsorption behavior of the designed
25 inhibitor was studied by kinetic and thermodynamic analyses.

26

27 **Methods.** Synthetic EPS is a bio-inspired material that was formulated based on the most typical
28 chemical compositions of natural WAS EPS, i.e. proteins, carbohydrates, humic substances,
29 nucleic acids, and uronic acids, which was not optimized for corrosion inhibition performance. It
30 is a mixture of glutamic acid, carboxymethylcellulose, humic acid, thymine, and alginic acid. Its
31 corrosion inhibition performance was tested with carbon steel in 3.64% NaCl saturated with
32 CO₂, using the potentiodynamic polarization scanning technique. The resulted electrochemical
33 parameters were used to evaluate the empirical corrosion kinetic and thermodynamic adsorption
34 parameters.

35

36 **Results.** Addition of synthetic EPS showed significant decrease in corrosion rate as compared to
37 the control. The inhibition efficiency improved with increasing inhibitor concentration and
38 temperature. The optimum performance was 94% with 204 mg/L of inhibitor applied at 70°C
39 (343 K). The inhibition performance was controlled by both the concentration of inhibitor and
40 temperature. Chemisorption of the inhibitor molecules contributed to the overall inhibition
41 performance, reducing the contact of metal with the corrosive environment, thus, slowing down
42 the overall corrosion rate.

43

44 Introduction

45 Extracellular polymeric substances (EPS) are the metabolic products produced by most
46 microorganisms. They accumulate on the surface of microorganisms, acting as protective
47 barriers against the microorganisms' external environment [1]. Typically, carbohydrates have
48 been identified as the major constituents in the EPS of many pure cultures [2][3], whereas
49 proteins were found in substantial quantities in the sludge of many wastewater treatment reactors
50 [1][4]. Small amounts of humic substances [5], uronic acids, and nucleic acids [1][6][7] were
51 also detected in EPS. A previous study [8][9] showed the potential of EPS extracted from waste
52 activated sludge (WAS) of wastewater treatment operations as a green corrosion inhibitor for
53 CO₂ corrosion. A maximum inhibition performance of about 80% was achieved with the
54 application of 1000 mg/L of this inhibitor. The corrosion inhibition mechanism of WAS EPS
55 was explained by the formation of a biofilm on the metal surface, shielding the metal surface
56 from the corrosive environment. Even though the inhibition performance is comparable to
57 commercial products, the nature of WAS caused inconsistency in inhibition efficiency. The
58 composition of WAS is dependent on wastewater treatment operational parameters, such as inlet
59 biochemical oxygen demand and sludge residence time.

60 This study focused on the evaluation of a corrosion inhibitor from the surrogate of WAS

61 EPS. The reason of making the surrogate was to have control on the chemical composition of the
62 corrosion inhibitor used and ensure consistent inhibition performance. This study hypothesized
63 that the designed synthetic EPS will demonstrate similar corrosion inhibition behavior as the
64 natural WAS EPS because it was formulated based on the major chemical compositions of
65 natural WAS EPS. The novelty of this research was the design of a surrogate biomass-based
66 corrosion inhibitor inspired by sources with varied chemical compositions. To the knowledge of
67 the authors, this line of work has not been reported elsewhere. This study is unique in the way
68 that it is a multidisciplinary work. Bio-inspired systems and materials are not uncommon in the
69 literature. Yet, this concept is the pioneer of the field of corrosion inhibitor formulation
70 development. For instance, some of the most commonly applied programming algorithms in
71 computer science and engineering today are bio-inspired. Algorithms like genetic and ant colony
72 mimic the natural biological systems to solve research problems. This study is adopting the bio-
73 inspired concept into the corrosion inhibitor formulation development. It is believed that this line
74 of multidisciplinary work could benefit and advance the research in corrosion inhibitor
75 development, especially the renewable type.

76 The present study seeks to investigate the corrosion inhibitive properties of synthetic EPS
77 for carbon steel in 3.64% NaCl solution saturated with CO₂ gas using the potentiodynamic
78 polarization technique. The corrosion kinetic parameters and thermodynamic adsorption
79 parameters are calculated and reported.

80

81 **Materials & Methods**

82 **Metal specimen preparation**

83 Potentiodynamic polarization scans were performed on carbon steels of the following
84 weight percentage composition: 0.17 C, 0.08 Mn, 0.014 P, 0.002 S, 0.022 Si, 0.02 Cu, 0.01 Ni,
85 0.04 Cr, 0.002 Sn, 0.042 Al, 0.006 N, 0.001 V, 0.0001 B, 0.001 Ti, 0.001 Cb, and the remainder
86 iron. The pre-treatment of the specimens' surface was carried out by grinding with sandpapers of
87 40, 220, 320 grits, rinsing with deionized water, then drying with paper towel. The specimens
88 were used immediately after pre-treatment.

89 **Corrosive medium preparation**

90 The corrosive medium was prepared with 36.4 g of NaCl (Fisher Scientific, Hampton,
91 NH, USA) in 1 L of deionized water to make up 3.64% of NaCl solution. The deionized water
92 used was drinking water filtered with Milli-Di Water Purification System (Merck Millipore,
93 Burlington, MA). Prior to starting of each experiment, CO₂ gas was sparged in the test solution
94 at 30 psi for 30 minutes. Then, the solution was transferred into the reactor, with CO₂ gas
95 continuously sparging throughout the experiment at 20 psi.

96 **Corrosion inhibitor preparation**

97 A mixture of several chemical compounds was labelled as synthetic EPS. It was used as
98 the test corrosion inhibitor in this study. The details of each compound, i.e. chemical type,
99 compound identity, vendor, specification, and composition, are listed in Table 1. These
100 compounds were mixed in the given composition as synthetic EPS. The concentrations of
101 inhibitors used in the following runs were doubled, tripled, and quadrupled.

102 Potentiodynamic polarization method

103 Potentiodynamic polarization experiments were carried out with Gamry Flexcell Critical
104 Pitting Cell Kit, connecting to the Gamry Potentiostat Interface 1000. The reference, counter,
105 and working electrodes used were saturated calomel electrode (SCE), graphite rod, and the metal
106 specimen, respectively. The setup was equipped with a heating jacket connected to TDC4
107 Omega temperature controller to maintain the test solution at a desired temperature, in this case,
108 25°C, 50°C, and 70°C. The Glas-Col GT Series stirrer was connected to the setup externally and
109 adjusted to 50 rpm to get the desired shear and to ensure even heating. The working solution
110 volume was 1 L. The working area of the metal specimens had a circular form of 5 cm².

111 The potentiodynamic polarization scans were carried out in potential range of -0.25 to
112 +0.25 V versus corrosion potential (E_{corr}) at a scan rate of 3 V/hr. Corrosive medium was added
113 into the reactor with carbon dioxide gas sparging constantly at 20 psi throughout the experiment.
114 The reactor was allowed to equalize for 30 minutes prior to the beginning of experiment. After
115 the system was equalized, Tafel plots were graphed with Gamry DC105 DC Corrosion
116 Technique Software until three relatively similar readings were obtained. Next, corrosion
117 inhibitor was added into the reactor. The reactor was again allowed to equalize for 30 minutes,
118 then Tafel plots were graphed. This step was repeated until three consecutive graphs with similar
119 trends were yielded, to ensure the stability of the system. Subsequently, the concentration of the
120 corrosion inhibitor was increased. Again, the system was being equalized for 30 minutes,
121 followed by the graphing of Tafel plots.

122 The Tafel plot was plotted with the mean values of corrosion potential (E_{corr}) and
123 corrosion current density (I_{corr}) from the triplicates of the experiments, while the electrochemical
124 parameters obtained from the curves were reported with mean and standard deviation. The
125 corrosion current densities were found by extrapolating the linear Tafel segment of the anodic
126 and cathodic curves to the corrosion potential. The corrosion inhibition efficiency was then
127 calculated with Equation 1.

$$128 \quad \text{Inhibition Efficiency (\%)} = \frac{I_{\text{corr, uninhibited}} - I_{\text{corr, inhibited}}}{I_{\text{corr, uninhibited}}} \times 100\% \quad (1)$$

129 Fourier-transform infrared spectroscopy (FTIR)

130 Agilent Cary 630 FTIR incorporated with MicroLab software were used for the FTIR
131 analysis in this study. This equipment worked based on Attenuated Total Reflection (ATR)
132 Method. The scanning was range between 4000 to 400 cm⁻¹ with resolution of 4 cm⁻¹.

133

134 Results

135 Corrosion inhibition performance

136 The Tafel plots generated from the potentiodynamic polarization measurements for
137 carbon steel in 3.64% NaCl saturated with CO₂ gas with synthetic EPS range from 51 mg/L to
138 204 mg/L at 25°C, 50°C, and 70°C (298 K, 323 K, 343 K) are presented in Figure 1, Figure 2,
139 and Figure 3, respectively. The details of electrochemical parameters obtained from the curves,
140 namely corrosion potential (E_{corr}), corrosion current density (I_{corr}), and inhibition efficiency, are
141 listed in Table 2. Moreover, the effects of inhibitor concentration and media temperature are

142 addressed in the discussion section. It is also worth noting that the significance of operation and
143 economics of the synthetic EPS as an oil field corrosion inhibitor formulation is also included in
144 the discussion section.

145 **Corrosion kinetic parameters**

146 Corrosion kinetic parameters, i.e. apparent activation corrosion energy (E_a), enthalpy of
147 activation (ΔH_a°), and entropy of activation (ΔS_a°), are listed in Table 3. Two Arrhenius plots
148 used for the evaluation of these corrosion kinetic parameters are shown in Figure 4 and Figure 5.
149 The details of calculations are discussed in the discussion section.

150 **Thermodynamic adsorption parameters**

151 The standard free energy of adsorption ($\Delta G_{\text{ads}}^\circ$), enthalpy of adsorption ($\Delta H_{\text{ads}}^\circ$), and the
152 entropy of adsorption ($\Delta S_{\text{ads}}^\circ$) are listed in Table 4. The Langmuir isotherm and the Van't Hoff
153 plots are shown in Figure 6 and Figure 7, respectively. The equations and graphs involved for the
154 thermodynamic adsorption parameters are explained in the discussion section.

155 **FTIR**

156 The IR spectra is shown in Figure 8 and the characteristic IR absorption frequencies of
157 the responding organic functional groups of synthetic EPS is tabulated in Table 5.

158

159 **Discussion**

160 **Properties of synthetic EPS**

161 Synthetic EPS is a mixture of several major groups of chemicals in natural WAS EPS.
162 Although there are many ways to extract EPS and each of the methods give different chemical
163 composition [1][7][10]; the composition of synthetic EPS formulated in this study will be based
164 on the method of heating. Typically, the EPS extracted by heating has the highest proteins
165 concentration, followed by carbohydrates, humic substances, nucleic acids, and uronic acids
166 [1][7][10]. Therefore, proteins will be the basis of the synthetic EPS and the ratio of different
167 chemicals will be based on the proteins. The compounds were mixed in ratios that were realistic
168 (small enough concentration to be able to measure accurately using an analytical balance) to be
169 acted as a corrosion inhibitor. They were mixed according to the following ratios:

- 170 a. Proteins:carbohydrates = 2.5:1
- 171 b. Proteins:humic substances = 6:1
- 172 c. Proteins:nucleic acids = 15:1
- 173 d. Proteins:uronic acids =15:1

174 In order for the synthetic EPS to resemble the natural WAS EPS while keeping the
175 complexity of the mixture low, one compound was selected from each chemical group. Since
176 five major groups are generally being studied in the natural WAS EPS, five components were
177 selected for the synthetic EPS formulation. They were chosen based on their structures and their
178 chemical inhibition performances in the literature. Structure wise, compounds with nitrogen,
179 oxygen, or sulfur atoms were preferred since all organic corrosion inhibitors typically contain at
180 least one of these atoms, almost without exception. In addition, bigger compounds are also
181 typically preferred as corrosion inhibitors because bigger compounds are more effective in

182 separating the metal surface from its corrosive environment when adsorbed on the metal surface.
183 The compounds chosen for the synthetic EPS mixture fulfilled these descriptions, as illustrated in
184 Figure 9. Furthermore, those chemicals that had demonstrated corrosion inhibition were
185 prioritized to be the candidates in the pool of selection. For protein, an amino acid, which is the
186 building block of a protein was chosen. Glutamic acid, a common component of bacterial cell
187 wall [11], made an excellent candidate as an amino acid for the purpose of this study since it has
188 also been proven to be an effective corrosion inhibitor in several studies [12][13]. Glutamic acid
189 showed approximately 54 to 90% of inhibition efficiency in 0.5 M HCl with copper [12][13].
190 Due to its potential in corrosion inhibition, it was chosen as the main component of the synthetic
191 EPS. The second biggest composition was carbohydrate. For an organic corrosion inhibitor,
192 typically, a bigger molecule is preferred. Carboxymethylcellulose (CMC), a relatively big
193 molecular weight packed with multiple oxygen atoms, was selected as the candidate for the
194 chemical group of carbohydrate. Its corrosion inhibition capability has also been proven
195 excellent in various investigations [14][15]. Inhibition efficiencies of about 65 to 72% were
196 observed when CMC was used with mild steel in acid solutions H_2SO_4 [14] and HCl [15],
197 respectively. However, corrosion inhibition studies on the rest of the chemical groups have no
198 record in the literature to date. For humic substances and uronic acids, there are not many
199 chemicals from these groups, so, humic acid and alginic acid were picked for each group,
200 respectively. In the case of nucleic acids, there are only four choices in this group, namely
201 thymine, guanine, adenine, and cytosine. Making a decision based on an economical point of
202 view, the most affordable choice was thymine. Thymine is a relatively smaller compound
203 compared to other chosen chemicals, but it contains both nitrogen and oxygen atoms, making it a
204 desirable option. Hence, glutamic acid, CMC, humic acid, thymine, and alginic acid were chosen
205 as the formulation for synthetic EPS. Their chemical structures are shown in Figure 9.

206 The formulation of synthetic EPS was designed solely based on the chemical composition
207 of natural WAS EPS, which was not optimized to meet the purpose of corrosion inhibition.
208 Interestingly, this corrosion inhibitor showed corrosion inhibition performance comparable to the
209 natural WAS EPS as well as commercial corrosion inhibitor. In order to improve the corrosion
210 inhibition efficiency of synthetic EPS, the future direction of the current research will focus on
211 optimizing the formulation to reduce the required applied concentration of corrosion inhibitor
212 while achieving the maximum attainable corrosion inhibition performance. This could be done
213 by first reducing the number of compounds in the formulation, followed by optimizing the
214 concentration of the compounds and the inhibition performance statistically.

215 The potential of utilizing biomass sources directly as corrosion inhibitors are undeniable.
216 There is an enormous amount of studies on the application of plant extracts as corrosion
217 inhibitors, but these products are still relatively rare in the market. One of the main reasons that
218 is delaying the commercialization of these inhibitors could be the current immature resource
219 recovery techniques. A lot of extraction methods are still economical infeasible these days.
220 Therefore, in order to promote the use of renewable corrosion inhibitors, as well as to improve
221 the marketability of these products, a bio-inspired corrosion inhibitor formulation is introduced
222 in this study. Compared to the traditional plant extracts corrosion inhibitors, this type of
223 renewable corrosion inhibitor is more market-ready because of several advantages: (1) renewable
224 sources, (2) economic feasibility, (3) chemical composition consistency, as well as (4) corrosion

225 inhibition performance consistency.

226 **Effect of concentration**

227 The curves in Figure 1, Figure 2, and Figure 3 revealed well defined anodic and cathodic
228 polarization Tafel regions. Note that only one set of experimental data was reported because the
229 differences in triplicates were insignificant. The results for the triplicates can be found in the raw
230 data section.

231 As observed in these figures, both cathodic and anodic reactions of carbon steel electrode
232 corrosion were inhibited by the increase concentration of synthetic EPS in 3.64% NaCl saturated
233 with CO₂ gas. This observation indicates that the addition of synthetic EPS reduced anodic
234 dissolution as well as the hydrogen evolution reaction [16]. This can be explained by the
235 adsorption of inhibitor over the corroded surface [17]. Tafel lines of nearly equal slopes were
236 obtained, indicating that the hydrogen evolution reaction was activated-controlled [18].

237 The details of electrochemical parameters obtained from the Tafel plots such as the
238 values of corrosion potential, E_{corr} , corrosion current density, I_{corr} , corrosion protection
239 efficiency, and surface coverage degree, θ , are presented in Table 2. The corrosion inhibition
240 efficiency was calculated using Equation 1, based on the I_{corr} values, where $I_{\text{corr,blank}}$ and I_{corr} were
241 the corrosion current density without and with inhibitor, respectively. These values were
242 obtained by the extrapolation of the cathodic and anodic Tafel lines to the corrosion potentials.
243 The data showed that the I_{corr} values decreased in the presence of synthetic EPS. These values
244 also dropped as the concentration of inhibitor increased, meaning that the corrosion reaction was
245 slowing down as the inhibitor concentration was increasing. This phenomenon can be attributed
246 to the adsorption of synthetic EPS on the metal surface [18].

247 There was no definite pattern observed in E_{corr} values in the presence of different
248 concentrations of synthetic EPS. This result indicated that synthetic EPS may be considered as a
249 mixed-type corrosion inhibitor [19] in the presence of CO₂ gas saturated 3.64% NaCl solution.
250 The maximum displacement in E_{corr} of less than 0.085 V suggests a mixed mode of inhibition
251 [20]. Mixed-type corrosion inhibitor retards corrosion rate by suppressing both anodic and
252 cathodic corrosion reactions, typically by adsorbing on a metal surface, forming a protective film
253 to reduce contact of metal surface from the corrosive environment [21].

254 The inhibition efficiency increased as the concentration of synthetic EPS increased. The
255 maximum inhibition was about 94% with an optimum inhibitor concentration of 204 mg/L at
256 70°C. At 25°C, the maximum inhibition protection of synthetic EPS was 82% at a concentration
257 of 153 mg/L. The previous study of WAS EPS inhibitor demonstrated an optimum inhibition
258 performance of about 79% at a concentration of 1000 mg/L [8]. Even though the inhibition
259 performance showed only a mere improvement of 3%, the inhibitor concentration was reduced
260 by about 6.5 times. It is known that the natural WAS EPS is rich in a variety of compounds.
261 These compounds could have posed steric hindrance on the adsorption of inhibition molecules
262 on the metal surface, bring down the efficiency of the overall inhibition performance, so, higher
263 concentrations of inhibitors were required to demonstrate the corrosion inhibition capability.
264 Unlike the natural WAS EPS, the synthetic EPS was formulated specifically on the EPS groups
265 that are known to perform as corrosion inhibitors. Hence, it is expected that the corrosion
266 inhibition efficiency of synthetic EPS to be higher than the natural WAS EPS. Furthermore, in
267 the case of commercial corrosion inhibitors, their corrosion protection performances are typically

268 above 70%. Synthetic EPS has a corrosion inhibition performance that is within the range of
269 commercial corrosion inhibitors. One advantage compared to natural WAS EPS is that its
270 inhibition performance is consistent. The results obtained from this study strongly suggest the
271 great potential commercialization value of synthetic EPS as a valuable material to inhibit
272 corrosion issues in oilfield operations.

273 **Effect of temperature**

274 The effect of temperature on the inhibited solution–metal reaction is highly complex
275 because many changes could occur on the metal surface such as rapid etching and desorption of
276 inhibitor, also, the inhibitor itself may undergo decomposition and/or rearrangement [22]. The
277 effect of corrosion inhibition by synthetic EPS in NaCl solution saturated with CO₂ gas was
278 studied with three different temperatures, i.e. 25°C, 50°C, and 70°C. Since the corrosion rate is
279 greatly affected by the concentration of inhibitor as well as the temperature of the working
280 environment, these factors have an important operational impact.

281 At different temperatures and inhibitor concentrations, the corrosion inhibition
282 efficiencies varied. It was apparent that the rates of carbon steel corrosion, both in the blank
283 solution of 3.64% NaCl saturated with CO₂ gas and with the presence of corrosion inhibitor,
284 increased with increasing temperature. The impact of temperature on the overall corrosion
285 reaction was more pronounced than the effect of inhibitor concentration. The inhibition
286 efficiency increased with temperature. Typically, a decrease in inhibition efficiency with a rise in
287 temperature suggests physisorption of the corrosion inhibitor. In contrast, an increase in
288 inhibition efficiency with rise in temperature is indicative of a chemisorption mechanism [23].
289 Therefore, the results clearly indicate a chemisorption mechanism of synthetic EPS on the carbon
290 steel surface.

291 **Corrosion kinetic parameters**

292 Corrosion kinetics parameters can be evaluated with different approaches. This study
293 seeks to quantitatively evaluate the performance of the studied corrosion inhibitor (synthetic
294 EPS) using an engineering calculation approach that yields empirical results. Instead of focusing
295 mechanistically on the chemistry of the corrosion and corrosion inhibitor reactions to obtain the
296 corrosion kinetics parameters, it is looking at an engineering perspective that is tailored to the
297 studied system. The chemistry of the corrosion and corrosion inhibitor reactions are unutterably
298 important, but it is not the center of the study. This study is not set up to investigate the
299 mechanistic values of the corrosion kinetic and thermodynamic adsorption parameters.

300 This paper emphasizes on the engineering significance of the synthetic EPS as a
301 corrosion inhibitor by applying engineering equations that are based on basic corrosion theory
302 but adapted heuristically to the studied system. Since the reported numbers (i.e. apparent
303 activation corrosion energy, enthalpy of activation, entropy of activation) are empirical values
304 that are only relevant to the studied system, these numbers may not be the duplicated with other
305 system set up (e.g. traditional weight loss method with beaker testing). Even though the reported
306 numbers are not the mechanistic values with respect to the theoretical corrosion reactions and the
307 theoretical adsorption of the inhibitors, it serves a purpose to screen the performance of the
308 studied corrosion inhibitor quantitatively using engineering calculations. In addition, the
309 empirical values are also helpful in determining the behavior of the inhibitor in the studied

310 system. For example, the enthalpy of activation could be used to describe whether the metal
 311 dissolution process is endothermic or exothermic. The idea is that, by adhering to the same
 312 experimental set up and procedure, the same engineering calculations can be performed to
 313 estimate the same parameters for other inhibitors, serving as a comparison model. This is a
 314 particularly valuable heuristic tool, where the corrosion inhibitor can be screened rapidly. Thus,
 315 if the results obtained from the experiment are encouraging, further corrosion testing such as
 316 sparged beaker test and wheel test could be considered. Furthermore, the same approach has
 317 previously been demonstrated in the literature [24][25], proven its usability and reliability.

318 The activation parameters for the corrosion reaction were calculated using an Arrhenius-
 319 type plot according to Equation 2. It is worth mentioning that the Arrhenius equations applied
 320 were tailored to the studied system, as a heuristic approach to estimate the empirical values of
 321 the apparent activation corrosion energy, enthalpy of activation, and entropy of activation that
 322 are true to the system. E_a in the equation denotes the apparent activation corrosion energy, R is
 323 the universal gas constant, and k is the Arrhenius pre-exponential factor. The values of apparent
 324 activation energy of corrosion were determined from the slope of $\ln I_{corr}$ versus $1/T$ plot, shown
 325 in Figure 4. The data showed lower activation energy in the presence of inhibitors than in its
 326 absence, which is a typical pattern of chemisorption [18].

327 An alternative formulation of Arrhenius equation, i.e. transition-state equation shown in
 328 Equation 3, was used to calculate the change of enthalpy (ΔH_a°) and entropy (ΔS_a°) of activation
 329 for the activation complex formation in the transition state. In this equation, the h is the Planck's
 330 constant, N is the Avagadro's number, ΔS_a° is the entropy of activation, and ΔH_a° is the enthalpy
 331 of activation. Figure 5 shows a plot of $\ln(I_{corr}/T)$ against $1/T$ for synthetic EPS. A straight line
 332 was obtained with a slope of $\Delta H_a^\circ/R$ and an intercept of $\ln(R/Nh + \Delta S_a^\circ/R)$, from which the
 333 values of ΔH_a° and ΔS_a° were calculated. The positive enthalpy values reflected the endothermic
 334 nature of metal dissolution process. Large and negative values of entropy imply that the activated
 335 complex in the rate determining step represents an association rather than a dissociation step
 336 [18].

$$337 \quad I_{corr} = k e^{-\frac{E_a}{RT}} \quad (2)$$

$$338 \quad I_{corr} = \frac{RT}{Nh} \exp\left(\frac{\Delta S_a^\circ}{R}\right) \exp\left(-\frac{\Delta H_a^\circ}{RT}\right) \quad (3)$$

339 Thermodynamic adsorption parameters

340 Adsorption isotherms provide insights into the interaction among the adsorbed molecules
 341 and the metal surface, which can help to better understand the corrosion inhibition mechanism.
 342 Similar to the corrosion kinetic parameters, the thermodynamic adsorption parameters reported
 343 in this section are only empirical values relevant to this studied system. The values of surface
 344 coverage (θ) to different concentrations of inhibitor, obtained from the polarization
 345 measurements in the temperature range of 25 to 70°C (298 to 343 K) were used to explain the
 346 best isotherm to determine the adsorption mechanism. The values of θ were assumed to be the
 347 corrosion inhibition efficiencies. The reason being, without the presence of inhibitor compound,
 348 an inhibition efficiency of 0% is expected, so, when an inhibitor compound is introduced to a
 349 corrosive environment, the improved corrosion inhibition efficiency is believed to be solely
 350 contributed by the coverage of the inhibitor compound on the metal surface. The surface

351 coverage, θ , were used in a series of equations shown in Equation 4, Equation 5, and Equation 6
 352 [26]. Equation 4 showed the relationship of I_{corr} , $I_{corr,blank}$, I_{sat} , and θ . I_{sat} is the current density of
 353 entirely covered surface. This equation was then be rearranged into Equation 5. As I_{corr} was
 354 greater than I_{sat} , Equation 5 was simplified to Equation 6.

$$355 \quad I_{corr} = (1 - \theta)I_{corr,blank} + \theta I_{sat} \quad (4)$$

$$356 \quad \theta = \frac{I_{corr,blank} - I_{corr}}{I_{corr,blank} - I_{sat}} \quad (5)$$

$$357 \quad \theta = \frac{I_{corr,blank} - I_{corr}}{I_{corr,blank}} \quad (6)$$

358 In the range of temperature and inhibitor concentration studied, the best correlation
 359 between the experimental results and the adsorption isotherm functions was obtained using
 360 Langmuir adsorption isotherm. The Langmuir isotherm for monolayer adsorption is given by
 361 Equation 7. By linearizing this equation, Equation 8 was obtained.

$$362 \quad \frac{\theta}{1 - \theta} = KC \quad (7) \quad \frac{C}{\theta} = \frac{1}{K} + C \quad (8)$$

363
 364 In Equation 7 and Equation 8, θ is the surface coverage degree, C is the inhibitor
 365 concentration in the NaCl solution, and K is the equilibrium constant of the adsorption process.
 366 The correlation coefficient, R^2 , was used to describe how close the isotherm fits the experimental
 367 data. The plot of C/θ against C gave a straight line and the linear correlation coefficients were
 368 fairly close to 1, indicating good fit to the data. This graph is shown in Figure 6. The adsorption
 369 behavior of synthetic EPS conformed to Langmuir isotherm, suggesting monolayer adsorption,
 370 which is a typical behavior of chemisorption [27].

371 In general, Langmuir isotherm is not recommended to be used to describe a mixture
 372 system because the individual components in a mixture can each be adsorbed in different ways.
 373 However, it is applicable to this study because the synthetic EPS, as a corrosion inhibitor
 374 formulation, was treated as an entity. The individual contribution of compounds in the mixture of
 375 synthetic EPS were considered unimportant, therefore, being omitted. These are the basic
 376 assumptions of Langmuir isotherm: (1) surface of the adsorbent (metal) is uniform, (2)
 377 adsorption sites are equivalent, (3) adsorbed molecules do not interact, (4) all adsorption occurs
 378 through the same mechanism. Assuming that the metal surface is uniform, the adsorption sites
 379 are equivalent, and the inhibitor formulation is being treated as an entity, Langmuir isotherm is
 380 appropriate to be used to describe the overall adsorption mechanism. There are numerous studies
 381 in the literature where Langmuir was used to describe the adsorption mechanism of an inhibitor
 382 mixture, especially plant extracts [28][29].

383 K values were calculated from the intercepts of the same plot (Figure 6). The constant of
 384 adsorption, K , can be related to the standard free energy of adsorption, ΔG°_{ads} , using Equation 9.
 385 The constant 1×10^6 in the equation is the concentration of water molecules expressed in mg/L,
 386 R is the universal gas constant, T is the absolute temperature. On the other hand, ΔH°_{ads} can be
 387 deduced from the integrated version of the Van't Hoff equation expressed by Equation 10.
 388 Figure 7 shows the plot of $\ln K$ versus $1/T$ which yield a straight line with a slope of $-\Delta H^\circ_{ads}/R$.

389 The value obtained was used to find the ΔH°_{ads} . The calculated ΔH°_{ads} was then used to calculate
 390 the values of ΔS°_{ads} by using Equation 11.

$$391 \quad \Delta G^\circ_{ads} = -RT \ln (1 \times 10^6 K) \quad (9)$$

$$392 \quad \ln K = -\frac{\Delta H^\circ_{ads}}{RT} + \frac{\Delta S^\circ_{ads}}{R} \quad (10)$$

$$393 \quad \Delta G^\circ_{ads} = \Delta H^\circ_{ads} - T\Delta S^\circ_{ads} \quad (11)$$

394 A more in-depth study of the inhibitor adsorption mechanism was investigated using the
 395 values of thermodynamic parameters. The details can be found in Table 4. The spontaneity of the
 396 adsorption of inhibitor on the metal surface as well as the stability of the adsorbed layer on the
 397 metal surface was demonstrated by the resulted negative values of ΔG°_{ads} . Typically, an
 398 endothermic adsorption process that has a positive value of ΔH°_{ads} is attributed unequivocally to
 399 chemisorption, while an exothermic adsorption process with ΔH°_{ads} of negative value may
 400 involve either physisorption or chemisorption, or a combination of both the processes [22]. In
 401 this study, the ΔH°_{ads} was positive, once again implying a chemisorption mechanism. The value
 402 of ΔS°_{ads} decreased with increased temperature, implying that the reaction of adsorption was
 403 getting less disordered.

404 FTIR

405 The corrosion inhibition capability of synthetic EPS was proven significant in this study.
 406 The trend in the IR spectrum of the synthetic EPS followed closely to the natural WAS EPS [8]
 407 as expected because it is formulated based on the chemical composition of natural WAS EPS.
 408 Similar to the natural WAS EPS, the FTIR results of synthetic EPS showed that functional
 409 groups O-H, N-H, C-N, C=O, and C-H were present. Since the synthetic EPS and natural WAS
 410 EPS both have the same functional group, it can be deduced that these functional groups play
 411 major roles in corrosion inhibition. Other authors have also suggested the contribution of these
 412 functional groups in corrosion inhibition [28][29].

413 This study treated the mixture of synthetic EPS as an entity, meaning that the
 414 contribution to the overall inhibition cannot be ascribed to any single component in the mixture.
 415 A suggestive corrosion inhibition mechanism of the synthetic EPS can be explained by the
 416 electrochemical theory. The electrochemical theory of corrosion holds that the metal surface
 417 corroding in an electrolyte is covered with local electrolytic cells. Some areas of the metal can
 418 act as anodes and other areas can act as cathodes, shown in Figure 10, depending upon the
 419 history of the metal regarding heat treatment, presence of imperfections, scratches, greases, paint
 420 coatings, fingerprint smudges, etc. At anodic sites, the metal usually dissolves into solution.
 421 Electrons given from these sites are transported to local cathodes and collected by electron
 422 acceptors such as hydrogen ions and oxygen. As previously suggested, synthetic EPS acts as a
 423 mixed-type corrosion inhibitor, meaning that the molecules in the synthetic EPS chemisorbed on
 424 both the anodic and cathodic sites of metal surface to form a monolayer protection film. The
 425 functional groups rich in nitrogen and oxygen atoms acted as the polar head of organic corrosion
 426 inhibitors, adsorbing on metal surface by forming chemical bonds between the inhibitor
 427 molecules and metal ions, while the non-polar hydrocarbon chain attached to the polar head
 428 isolated the metal surface from the corrosive surrounding, suppressing both anodic and cathodic
 429 corrosion reactions, reducing the overall corrosion rate.

430

431 **Engineering, operation, and economic significance of synthetic EPS**

432 The corrosion inhibition performance of the synthetic EPS shown in this study is
433 promising. Other areas that are interesting to be investigated are the engineering, operational, and
434 economical sides of this corrosion inhibitor formulation.

435 This article is an extension of a previous study that showed the potential of EPS extracted
436 from waste activated sludge (WAS) of wastewater treatment operations as a green corrosion
437 inhibitor for CO₂ corrosion. A maximum inhibition performance of about 80% was achieved
438 with the application of 1000 mg/L of this inhibitor [8][9]. The major flaw in this corrosion
439 inhibitor is that the inhibition performance is not consistent due to the variation in wastewater
440 compositions. Thus, synthetic EPS was formulated in this study based on the natural composition
441 of WAS EPS, as a bio-inspired material, that resemble the inhibition performance of natural
442 WAS EPS, but with consistent inhibition performance. This approach is novel in research and
443 development of green corrosion inhibitor development. Commercial corrosion inhibitor for the
444 oil and gas industry are generally petroleum-based, while most green corrosion inhibitors
445 reported in the literature were directly extracted from agricultural sources. The technique used in
446 this study for the development of bio-inspired material as a corrosion inhibitor can be further
447 expanded in the area of green corrosion inhibitors development and potentially be extended to
448 other research fields.

449 In terms of operation significance, similar to most bio-inspired materials, this corrosion
450 inhibitor formulation can be formulated with commercial renewable resources or extracted from
451 natural resources (waste activated sludge), leaving a lesser environmental impact compared to
452 the commercial petroleum-based corrosion inhibitors. Besides having corrosion inhibition
453 performance comparable to commercial products (commercial products usually show inhibition
454 performance above 70%), the synthetic EPS is also just as easy to be applied like commercial
455 corrosion inhibitors, making it an excellent alternative.

456 The economic analysis of synthetic EPS was evaluated in this study. The production cost
457 of the synthetic EPS is about \$4.23 for every 10,000-inhibition treatment (assuming 1 L
458 system/treatment), while the market price of a typical commercial oil and gas corrosion inhibitor
459 costs about \$2.38 per 10,000 applications. It is worth mentioned that the synthetic EPS is
460 formulated based solely on the composition of natural EPS. The economic feasibility can be
461 improved in future studies by product optimization to reduce the applied inhibitor concentration
462 and enhance the inhibition performance.

463 It is evident that bio-inspired systems/materials have high potential in revolutionizing the
464 current market to reduce dependence on fossil fuel-based products as well as to promote
465 innovative product development approach. This transformation is not only applicable in the
466 corrosion inhibitor industry but should also be extended to benefit other research and
467 development areas.

468

469 **Conclusions**

470 The studied corrosion inhibitor, synthetic EPS, showed corrosion inhibition capability for
471 carbon steel when tested in 3.64% NaCl saturated with CO₂ gas. Synthetic EPS is a surrogate of
472 biomass-based corrosion inhibitor inspired by sources with varied chemical compositions to
473 overcome the composition inconsistency in biomass that can cause unreliable corrosion
474 inhibition performance. Synthetic EPS is a mixture of glutamic acid, carboxymethylcellulose,
475 humic acid, thymine, and alginic acid, following the chemical composition of natural WAS EPS
476 extracted by heating method. Unlike the natural WAS EPS that is rich in assorted of molecules
477 that could promote steric hindrance on the adsorption of inhibitor molecules, synthetic EPS was
478 designed specifically based on the EPS groups that are known to perform as corrosion inhibitors.
479 The electrochemical testing used in this study showed that the corrosion rates were significantly
480 reduced with the addition of synthetic EPS. With concentration of 204 mg/L in 3.64% NaCl
481 saturated with CO₂ gas, synthetic EPS showed maximum corrosion inhibitions of 82.41%,
482 89.65%, and 93.99% at 25°C, 50°C, and 70°C, respectively. Its performance compared favorably
483 with natural WAS EPS and commercial corrosion inhibitors. It was found that the inhibition
484 performance was controlled by both the concentration of inhibitor and temperature.

485 The corrosion inhibition capability was due to chemisorption shown by several
486 evidences:

- 487 (1) An increase in corrosion inhibition efficiency with increase temperature
- 488 (2) A decrease in activation energy in the presence of inhibitor
- 489 (3) Endothermic adsorption

490 Since the formulation of synthetic EPS was designed solely based on the chemical
491 composition of natural WAS EPS, it was not optimized to meet the purpose of corrosion
492 inhibition. Based on the results presented and the needs and requirements of corrosion protection
493 service providers, the future direction of the current research will focus on optimizing the
494 formulation in order to reduce the required applied concentration of corrosion inhibitor while
495 achieving the maximum attainable corrosion inhibition performance. This could be done by first
496 reducing the number of compounds in the formulation, then optimizing the concentration of the
497 compounds and the inhibition performance statistically.

498 This bio-inspired material is developed in the hope to promote the commercialization of
499 renewable corrosion inhibitors. According to the Google Scholar database, there are as many as
500 17,600 publications on the topic of green corrosion inhibitors from the year 1980 to 2018. A
501 significant portion of these publications were made up by phytochemical-based compounds.
502 Plant extracts are gaining popularity as green corrosion inhibitors candidates not only because
503 they are renewable sources, but also their potential in corrosion mitigation. On average, the
504 attainable corrosion protection efficiencies of these inhibitors can range from 70% to as high as
505 98% [30][31][32][33][34]. Despite the overwhelming research evidence that suggests the
506 impressive performance of these inhibitors, there are still drastic uneven numbers of research
507 reports and products on the shelves. Needless to say, resource recovery efforts take time to
508 improve. Before these techniques are optimized, or if there are enough products to be added to
509 the product line to improve the cost issue [35], until then, bio-inspired material could be an

510 alternative to balance the environmental problems bring by petroleum-based corrosion inhibitors
511 and the economic complications raise by plant extracts corrosion inhibitors. As a matter of
512 course, the idea of benefiting from bio-inspired systems and materials will not only benefit the
513 corrosion inhibitor sector but is prompt to be extended to any other applicable research area.

514 **References**

- 515 [1] H. Liu and H. H. P. Fang, "Extraction of extracellular polymeric substances (EPS) of
516 sludges," *J. Biotechnol.*, vol. 95, no. 3, pp. 249–256, 2002.
- 517 [2] P. Cescutti, R. Toffanin, P. Pollesello, and I. W. Sutherland, "Structural determination of
518 the acidic exopolysaccharide produced by a *Pseudomonas* sp. strain 1.15," *Carbohydr.*
519 *Res.*, vol. 315, no. 1, pp. 159–168, 1999.
- 520 [3] L. Kennedy and I. W. Sutherland, "Polysaccharide lyases from gellan-producing
521 *Sphingomonas* spp.," *Microbiology*, vol. 142, no. 4, pp. 867–872, Apr. 1996.
- 522 [4] M. C. Veiga, M. K. Jain, W. Wu, R. I. Hollingsworth, and J. G. Zeikus, "Composition and
523 role of extracellular polymers in methanogenic granules.," *Appl. Environ. Microbiol.*, vol.
524 63, no. 2, pp. 403–407, 1997.
- 525 [5] B. F. Nielsen, T. Griebe, and P. H. Nielsen, "Enzymatic activity in the activated-sludge
526 floc matrix," *Appl. Microbiol. Biotechnol.*, vol. 43, no. 4, pp. 755–761, 1995.
- 527 [6] H. Ji, "Polymerization of humic substances in natural environments," in *Humic substances*
528 *and their role in the environment*, Chichester: Wiley, 1988, pp. 45–58.
- 529 [7] B. Frølund, R. Palmgren, K. Keiding, and P. H. Nielsen, "Extraction of extracellular
530 polymers from activated sludge using a cation exchange resin," *Water Res.*, vol. 30, no. 8,
531 pp. 1749–1758, 1996.
- 532 [8] L. C. Go, W. Holmes, D. Depan, and R. Hernandez, "Evaluation of extracellular
533 polymeric substances extracted from waste activated sludge as a renewable corrosion
534 inhibitor," *PeerJ*, vol. 7, p. e7193, Jun. 2019.
- 535 [9] L. C. Go, W. Holmes, and R. Hernandez, "Sweet corrosion inhibition on carbon steel
536 using waste activated sludge extract," in *2019 IEEE Green Technologies*
537 *Conference(GreenTech)*, 2019, pp. 1–4.
- 538 [10] S. Comte, G. Guibaud, and M. Baudu, "Relations between extraction protocols for
539 activated sludge extracellular polymeric substances (EPS) and EPS complexation
540 properties: Part I. Comparison of the efficiency of eight EPS extraction methods," *Enzyme*
541 *Microb. Technol.*, vol. 38, no. 1, pp. 237–245, 2006.
- 542 [11] D. S. Hoare, "The breakdown and biosynthesis of glutamic acid," *J. Gen. Microbiol.*, vol.
543 32, no. 2, pp. 157–161, Aug. 1963.
- 544 [12] D.-Q. Zhang, Q.-R. Cai, L.-X. Gao, and K. Y. Lee, "Effect of serine, threonine and
545 glutamic acid on the corrosion of copper in aerated hydrochloric acid solution," *Corros.*
546 *Sci.*, vol. 50, no. 12, pp. 3615–3621, 2008.
- 547 [13] D.-Q. Zhang, Q.-R. Cai, X.-M. He, L.-X. Gao, and G.-D. Zhou, "Inhibition effect of some
548 amino acids on copper corrosion in HCl solution," *Mater. Chem. Phys.*, vol. 112, no. 2,
549 pp. 353–358, 2008.
- 550 [14] M. M. Solomon, S. A. Umoren, I. I. Udosoro, and A. P. Udoh, "Inhibitive and adsorption
551 behaviour of carboxymethyl cellulose on mild steel corrosion in sulphuric acid solution,"
552 *Corros. Sci.*, vol. 52, no. 4, pp. 1317–1325, 2010.

- 553 [15] E. BAYOL, A. GURTEN, M. DURSUN, and K. KAYAKIRILMAZ, “Adsorption
554 Behavior and Inhibition Corrosion Effect of Sodium Carboxymethyl Cellulose on Mild
555 Steel in Acidic Medium,” *Acta Physico-Chimica Sin.*, vol. 24, no. 12, pp. 2236–2243,
556 Dec. 2008.
- 557 [16] M. S. Morad, “Inhibition of phosphoric acid corrosion of zinc by organic onium
558 compounds and their adsorption characteristics,” *J. Appl. Electrochem.*, vol. 29, pp. 619–
559 626, 1999.
- 560 [17] M. Abdallah, “Guar Gum as Corrosion Inhibitor for Carbon Steel in Sulfuric Acid
561 Solutions,” *Port. Electrochim. Acta*, vol. 22, pp. 161–175, 2004.
- 562 [18] M. Bouklah, B. Hammouti, M. Lagrenée, and F. Bentiss, “Thermodynamic properties of
563 2,5-bis(4-methoxyphenyl)-1,3,4-oxadiazole as a corrosion inhibitor for mild steel in
564 normal sulfuric acid medium,” *Corros. Sci.*, vol. 48, no. 9, pp. 2831–2842, 2006.
- 565 [19] Harish Kumar and Vikas Yadav, “Citrus sinensis peels as a Green Corrosion Inhibitor for
566 Mild Steel in 5.0 M Hydrochloric Acid Solution,” *Res. J. Chem. Sci.*, vol. 6, no. 1, pp. 53–
567 60, 2016.
- 568 [20] N. Chaubey, V. K. Singh, and M. A. Quraishi, “Effect of some peel extracts on the
569 corrosion behavior of aluminum alloy in alkaline medium,” *Int. J. Ind. Chem.*, vol. 6, no.
570 4, pp. 317–328, Nov. 2015.
- 571 [21] R. Myrdal, “Corrosion Inhibitors– State of the art,” 2010.
- 572 [22] F. Bentiss, M. Lebrini, and M. Lagrenée, “Thermodynamic characterization of metal
573 dissolution and inhibitor adsorption processes in mild steel/2,5-bis(n-thienyl)-1,3,4-
574 thiadiazoles/hydrochloric acid system,” *Corros. Sci.*, vol. 47, no. 12, pp. 2915–2931,
575 2005.
- 576 [23] A. Popova, E. Sokolova, S. Raicheva, and M. Christov, “AC and DC study of the
577 temperature effect on mild steel corrosion in acid media in the presence of benzimidazole
578 derivatives,” *Corros. Sci.*, vol. 45, no. 1, pp. 33–58, 2003.
- 579 [24] F. S. de Souza and A. Spinelli, “Caffeic acid as a green corrosion inhibitor for mild steel,”
580 *Corros. Sci.*, vol. 51, no. 3, pp. 642–649, Mar. 2009.
- 581 [25] A. Al-Amiery, A. Kadhum, A. Kadhum, A. Mohamad, C. How, and S. Junaedi,
582 “Inhibition of Mild Steel Corrosion in Sulfuric Acid Solution by New Schiff Base,”
583 *Materials (Basel)*, vol. 7, no. 2, pp. 787–804, Jan. 2014.
- 584 [26] E. Khamis, “The Effect of Temperature on the Acidic Dissolution of Steel in the Presence
585 of Inhibitors,” *Corrosion*, vol. 46, no. 6, pp. 476–484, 1990.
- 586 [27] “Thermodynamics and Kinetics of Adsorption.” [Online]. Available: http://w0.rz-berlin.mpg.de/imprs-cs/download/Vortrag_IMPRS_Schmoekwitz_Mi_9-11_KChrist.pdf.
587
- 588 [28] E. E. Ebenso, N. O. Eddy, and A. O. Odiongenyi, “Corrosion inhibitive properties and
589 adsorption behaviour of ethanol extract of Piper guinensis as a green corrosion inhibitor
590 for mild steel in H₂SO₄,” *African J. Pure Appl. Chem.*, vol. 2, no. 11, pp. 107–115, 2008.

- 591 [29] E. I. Ating, S. A. Umoren, I. I. Udousoro, E. E. Ebenso, and A. P. Udoh, "Leaves extract
592 of *Ananas sativum* as green corrosion inhibitor for aluminium in hydrochloric acid
593 solutions," *Green Chem. Lett. Rev.*, vol. 3, no. 2, pp. 61–68, Jun. 2010.
- 594 [30] N. O. Eddy and E. E. Ebenso, "Adsorption and inhibitive properties of ethanol extracts of
595 *Musa sapientum* peels as a green corrosion inhibitor for mild steel in H₂SO₄," *African J.*
596 *Pure Appl. Chem.*, vol. 2, no. 6, pp. 46–54, 2008.
- 597 [31] Taleb H. Ibrahim, Youssef Chehade, and Mohamed Abou Zour, "Corrosion Inhibition of
598 Mild Steel using Potato Peel Extract in 2M HCl Solution," *Int. J. Electrochem. Sci.*, vol. 6,
599 pp. 6542–6556, 2011.
- 600 [32] H. Elmsellem, H. Bendaha, A. Aouniti, A. Chetouani, M. Mimouni, and A. Bouyanzer,
601 "Comparative study of the inhibition of extracts from the peel and seeds of *Citrus*
602 *Aurantium* against the corrosion of steel in molar HCl solution," *Moroccan J. Chem.*, vol.
603 2, no. 1, pp. 1–9, 2014.
- 604 [33] Janaina Cardozo da Rocha, José Antônio da Cunha Ponciano Gomes, and Eliane D'Elia,
605 "Aqueous extracts of mango and orange peel as green inhibitors for carbon steel in
606 hydrochloric acid solution," *Mater. Res.*, vol. 17, no. 6, pp. 1516–1439, 2014.
- 607 [34] M. Sangeetha, S. Rajendran, J. Sathiyabama, and P. Prabhakar, "Eco friendly extract of
608 Banana peel as corrosion inhibitor for carbon steel in sea water," *J. Nat. Prod. Plant*
609 *Resour.*, vol. 2, no. 5, pp. 601–610, 2012.
- 610 [35] L. C. Go, D. L. Fortela, E. Revellame, M. Zappi, W. Chirdon, W. Holmes, and R.
611 Hernandez, "Biobased chemical and energy recovered from waste microbial matrices,"
612 *Curr. Opin. Chem. Eng.*, vol. 26, pp. 65–71, Dec. 2019.

613

614

615

Table 1 (on next page)

Details of synthetic EPS

Type	Chemical	Vendor	Specification	Amount (mg/L)
Protein	Glutamic acid	Acros Organics	99%	30
Carbohydrate	Carboxymethyl cellulose (CMC)	Acros Organics	MW 70,000	12
Humic acid	Humic acid	Acros Organics	45-70%	5
Nucleic acid	Thymine	Alfa Aesar	97%	2
Uronic acid	Alginic acid, sodium salt	Acros Organics	-	2

1

Table 2 (on next page)

Electrochemical parameters and the corresponding corrosion inhibition efficiencies in the presence of different concentrations of synthetic EPS at various temperatures

Temperature (°C)	Temperature (K)	Concentration (mg/L)	E_{corr} (V)	I_{corr} ($\mu\text{A}/\text{cm}^2$)	Inhibition efficiency (%)	Surface coverage degree, θ
25	298	0	-0.73	52.48	-	-
		51	-0.71	25.12	68.72	0.6872
		102	-0.71	18.20	77.34	0.7734
		153	-0.71	14.45	82.00	0.8200
		204	-0.70	14.13	82.41	0.8241
50	323	0	-0.74	125.89	-	-
		51	-0.76	37.15	86.03	0.8603
		102	-0.76	34.67	86.96	0.8696
		153	-0.76	33.11	87.55	0.8755
		204	-0.76	27.54	89.65	0.8965
70	343	0	-0.73	223.87	-	-
		51	0.76	45.71	91.70	0.9170
		102	-0.76	39.81	92.77	0.9277
		153	-0.76	34.67	93.71	0.9371
		204	0.75	33.11	93.99	0.9399

1

Table 3 (on next page)

Corrosion kinetic parameters for carbon steel in different concentrations of the synthetic EPS

Inhibitor concentration (mg/L)	E _a (kJ/mol)	ΔH _a ^o (kJ/mol)	ΔS _a ^o (J/mol K)
0	27.46	24.81	-71.28
51	12.54	8.75	-131.24
102	15.21	12.56	-120.83
153	17.24	14.59	-115.63
204	16.47	13.82	-118.73

1

Table 4(on next page)

Thermodynamic parameters for the adsorption of synthetic EPS at different temperatures

Temperature (°C)	Temperature (K)	R ²	K ([mg/L] ⁻¹)	$\Delta G_{\text{ads}}^{\circ}$ (kJ/mol)	$\Delta H_{\text{ads}}^{\circ}$ (kJ/mol)	$\Delta S_{\text{ads}}^{\circ}$ (J/mol K)
25	298	0.9980	0.01039	-22.93	7.5192	102.11
50	323	0.9969	0.01325	-23.53		72.81
70	343	0.9999	0.01545	-23.91		69.68

1

Table 5 (on next page)

Characteristic IR absorption frequencies of organic functional groups

Characteristic Absorptions (cm ⁻¹)	Vibration Type	Functional Type
3,200 - 3,600	Phenol OH stretch	OH into polymeric compounds
2,850 - 3,000	Alkane C-H stretch	
1,690 - 1,630	Amide C=O stretch	Proteins
1,590 - 1,650	Amide (I) N-H bend	
1,500 - 1,560	Amide (II) N-H bend	
1,350 - 1,480	Alkane C-H bending	
1,080 - 1,360	Amine C-N stretch	

1

Figure 1

Tafel plot for carbon steel in 3.64% NaCl concentrated with CO₂ with different concentrations of synthetic EPS at 25°C

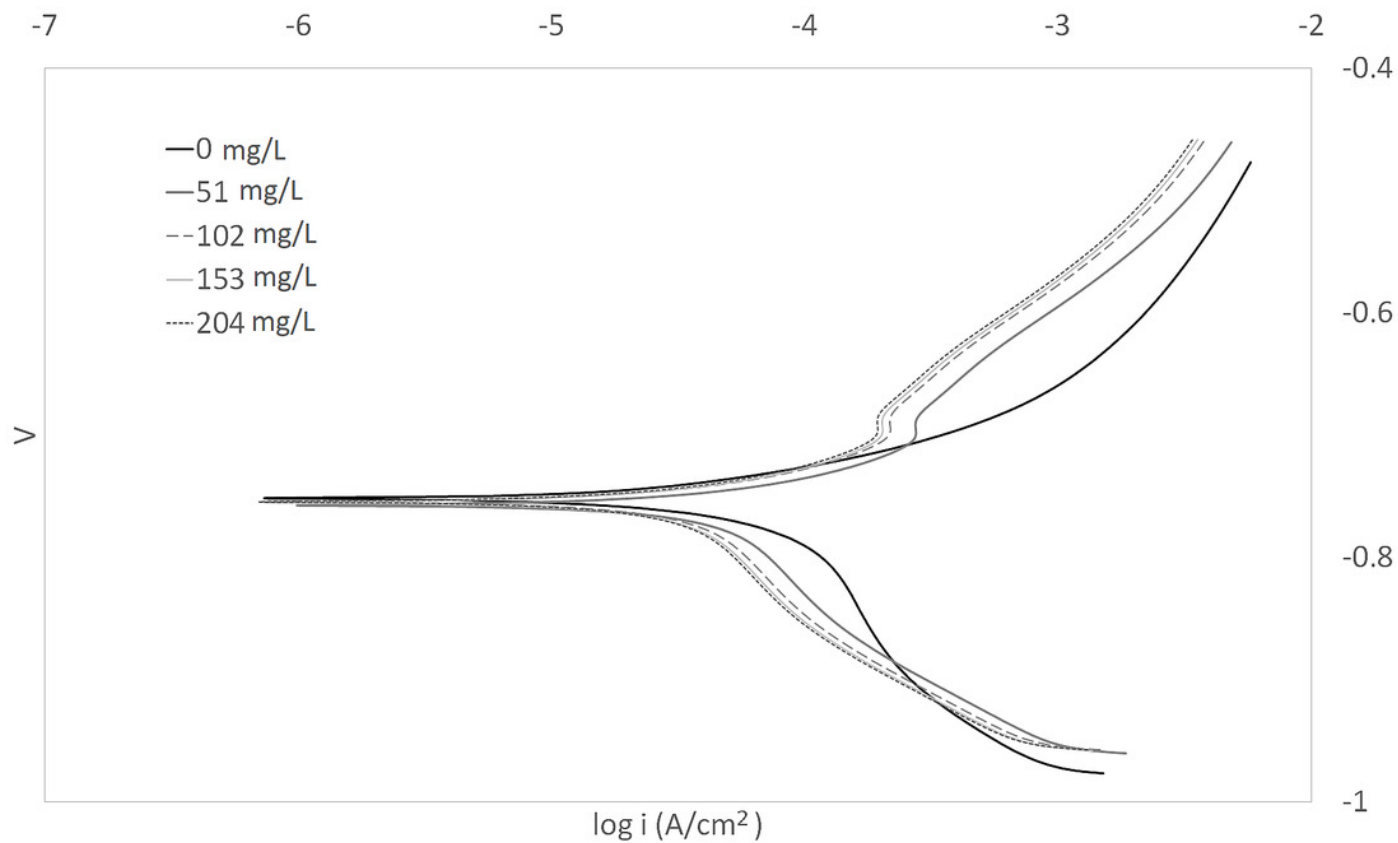


Figure 2

Tafel plot for carbon steel in 3.64% NaCl concentrated with CO₂ with different concentrations of synthetic EPS at 50°C

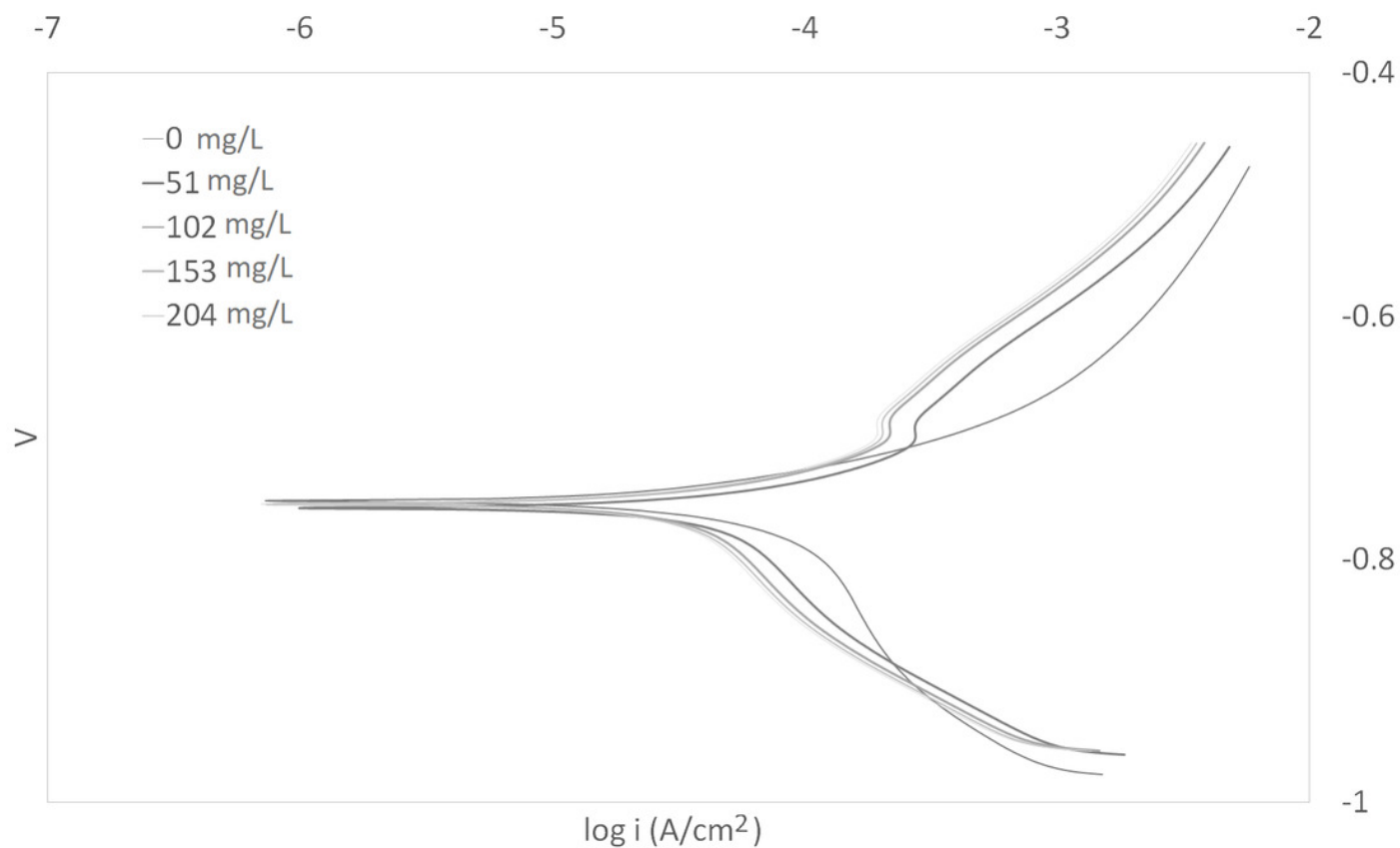


Figure 3

Tafel plot for carbon steel in 3.64% NaCl concentrated with CO₂ with different concentrations of synthetic EPS at 70°C

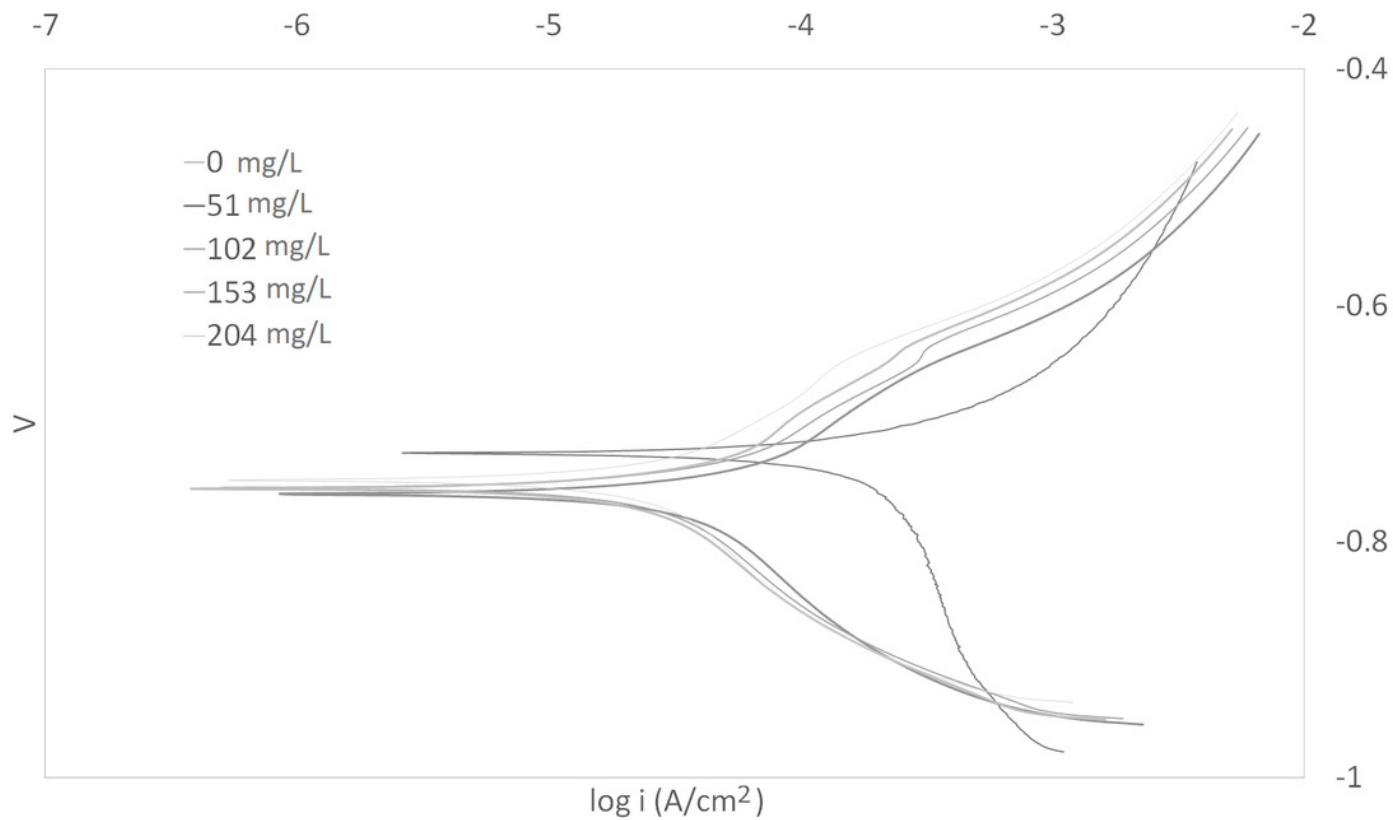


Figure 4

Arrhenius plots of $\ln I_{\text{corr}}$ versus $1/T$ at different concentrations of synthetic EPS

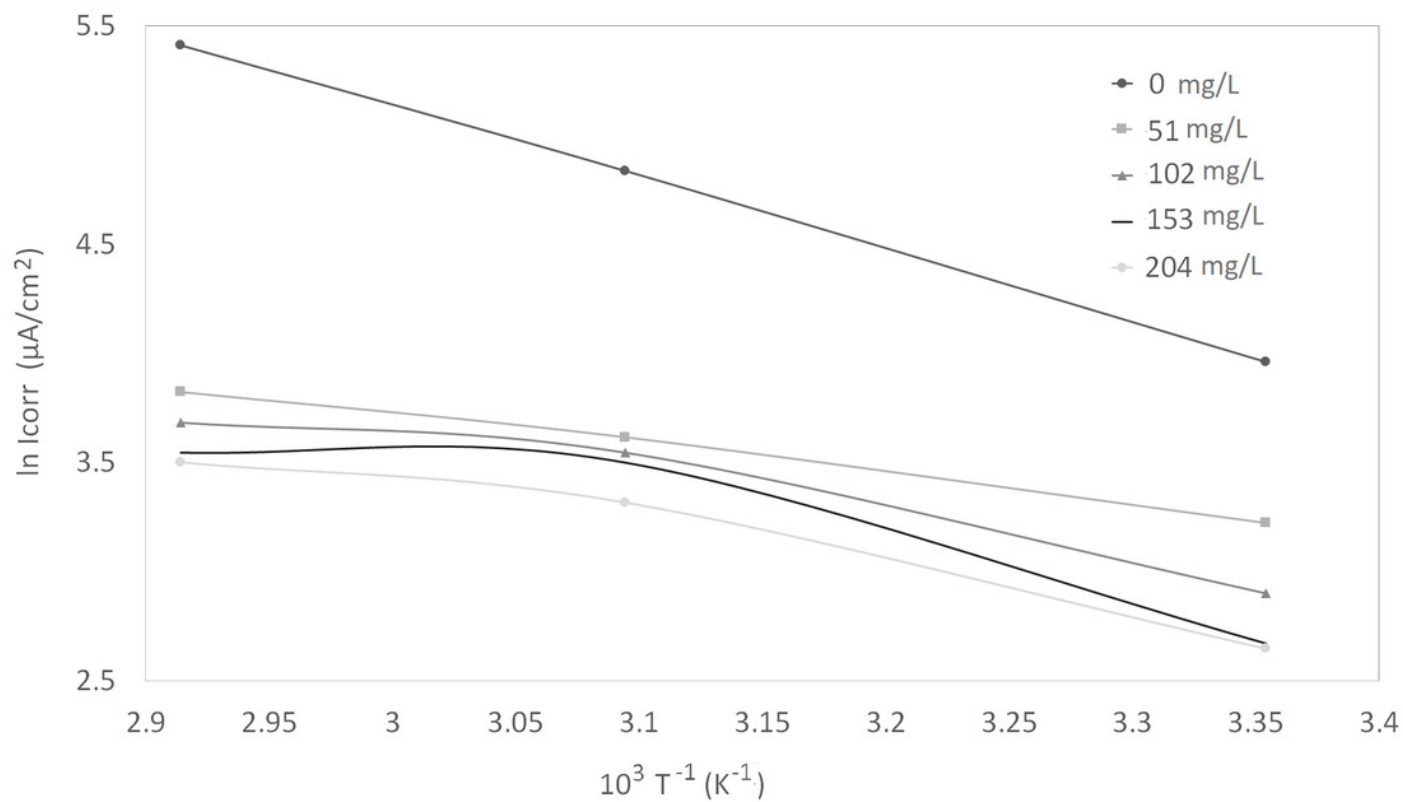


Figure 5

Arrhenius plots of corrosion $\ln(I_{\text{corr}}/T)$ versus $1/T$ at different concentrations of synthetic EPS

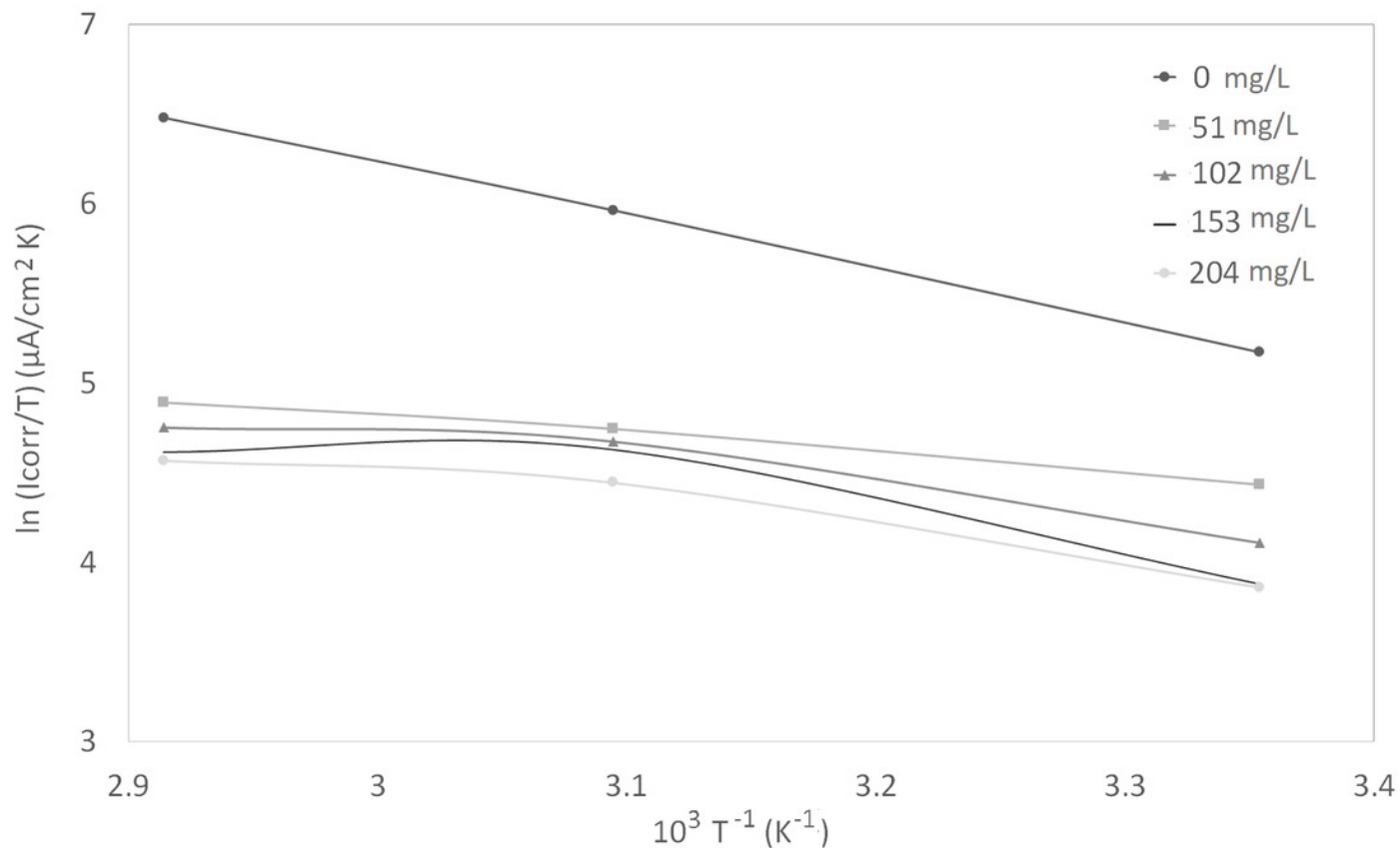


Figure 6

Curve fitting of the experimental data to Langmuir isotherm

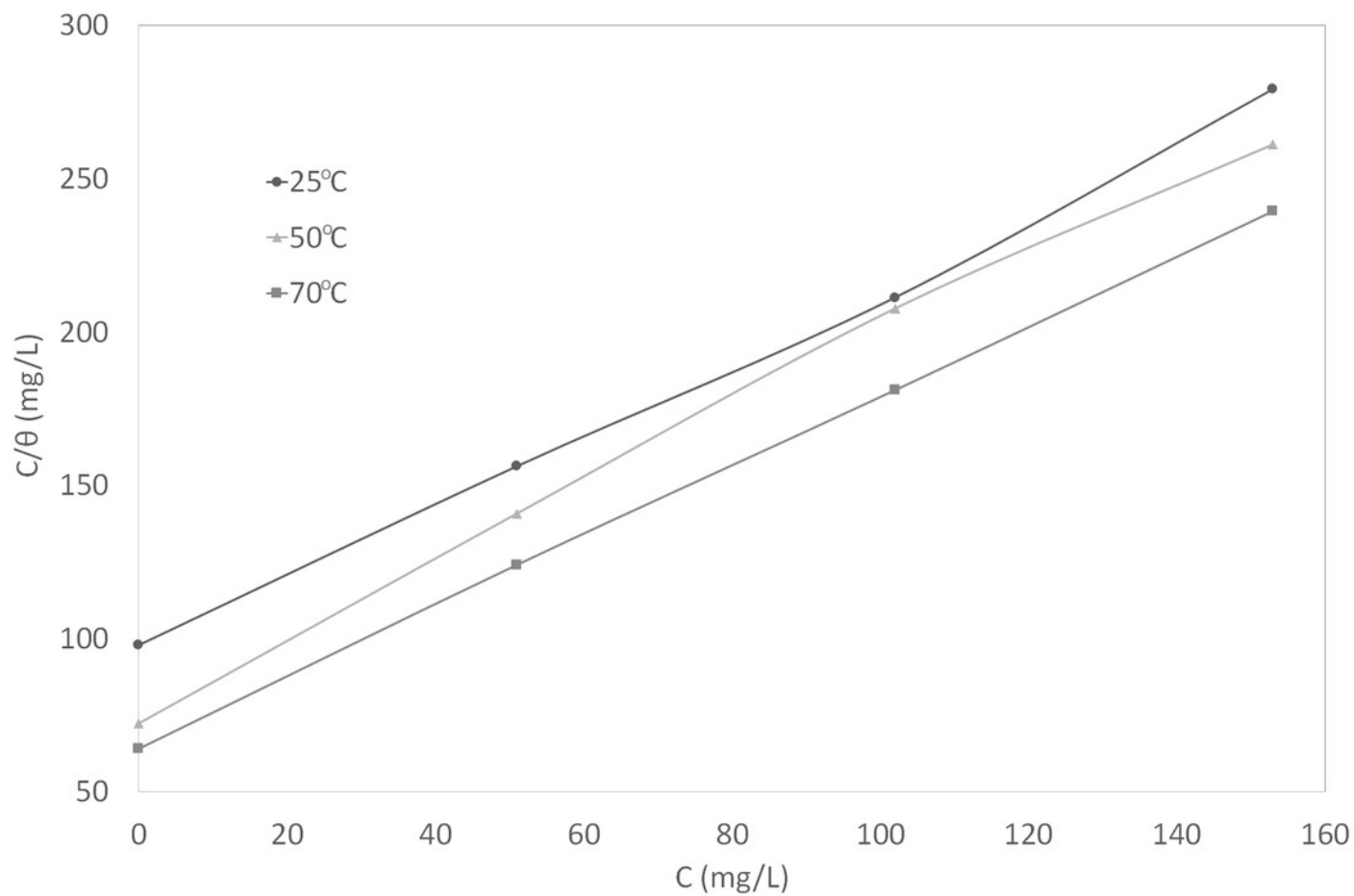


Figure 7

Van't Hoff plot

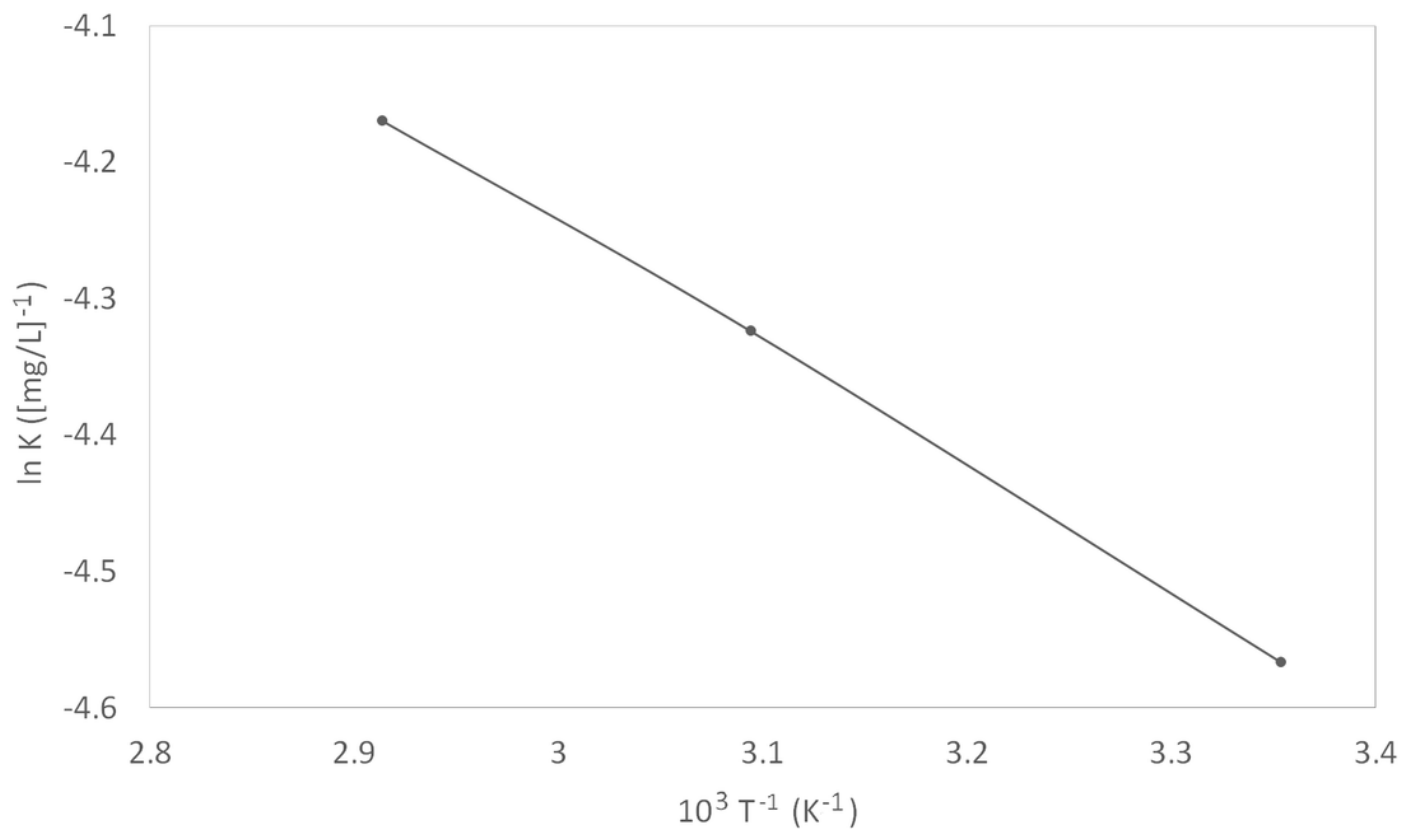


Figure 8

IR spectra of synthetic EPS

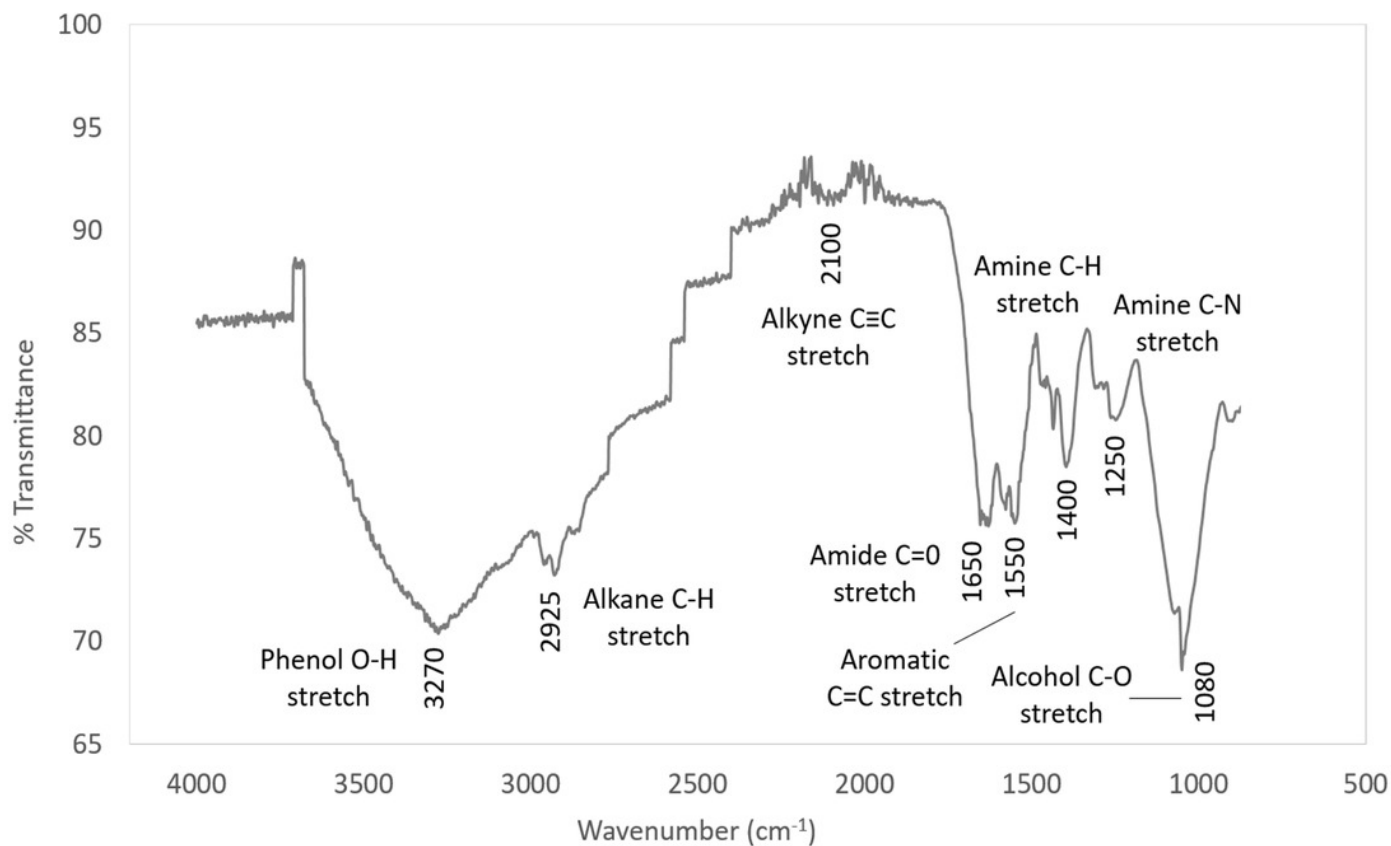


Figure 9

Chemicals in synthetic EPS and their structures

(a) Protein: Glutamic acid. (b) Carbohydrate: Carboxymethylcellulose. (c) Humic substances: Humic acid. (d) Nucleic acid: Thymine. (e) Uronic acid: Alginic acid.

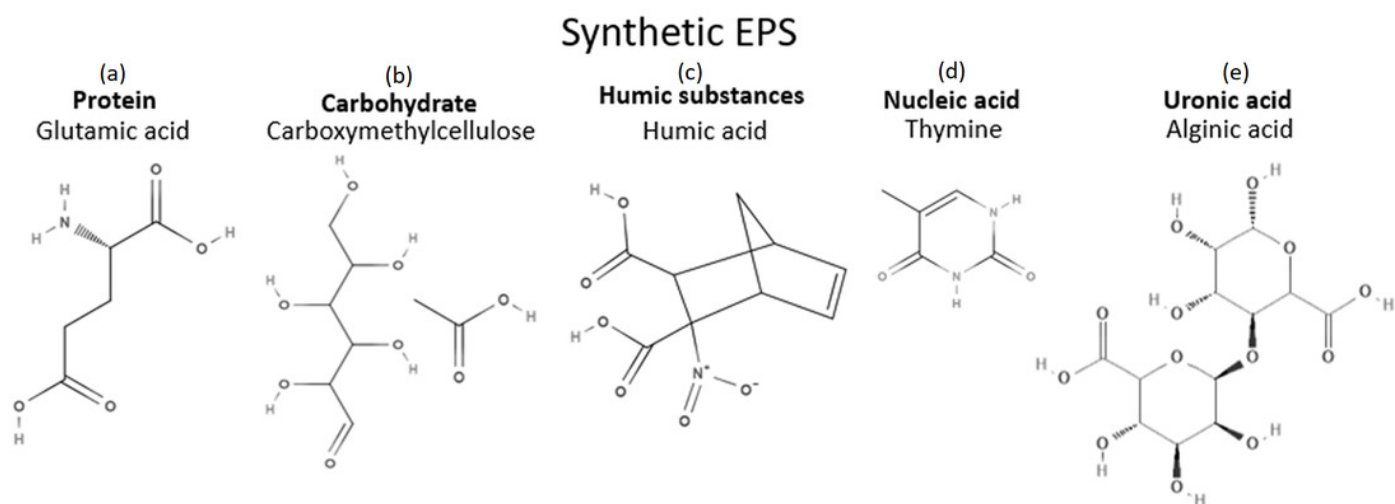


Figure 10

Corrosion inhibition mechanism of synthetic EPS

I: Inhibitor

